International Journal of Fracture, Vol. 11, No. 4, August 1975
Noordhoff International Publishing–Leyden
Printed in The Netherlands

The calculation of stress intensity factors for combined tensile and shear loading

T. K. HELLEN

Central Electricity Generating Board, Berkeley Laboratories, Berkeley, Gloucestershire, England

W. S. BLACKBURN

C. A. Parsons & Co. Ltd., Heaton Works, Newcastle upon Tyne, England

(Received November 9, 1973)

ABSTRACT

Stress intensity calculations are presented for cases of combined tensile and shear loading for a linear elastic material. Using functions of a complex variable, a theory is developed to determine the direction of maximum energy release rate. A finite element method using virtual crack extensions is also used to determine the energy release rate for crack extensions in various directions and in particular that which gives the maximum energy release rate.

Except when shear is more significant than tension, these results give good agreement with available experimental evidence. When shear is most significant, plasticity effects are probably becoming important, thereby invalidating the results of any linear theory. However, the results may still be used to determine K_I and K_{II} numerically from virtual crack extension calculations of J_1 and J_2 for general two-dimensional geometries.

1. Introduction

The main aim of fracture investigations is to be able to predict the size of crack which will propagate under a given loading in a given material, from measurements of the size of crack which propagates under another loading in the same material, temperature and environment. The relationships between these sizes is dependent on the conditions near the tip of the crack, where non-elastic effects are significant. However, provided that such a region is small compared with the crack dimensions, a linear elastic stress field may be assumed around the crack tip. In these circumstances, the onset of fracture is controlled by the magnitude of the stress intensity factors K_I, K_{II} and K_{III} (relating to tensile, in-plane shear, and out-of-plane shear respectively). These are the coefficients of $r^{-\frac{1}{2}}$ in the singular part of the expansion of the stresses ahead of the crack as a function of r, the distance from the tip.

For arbitrary cracked geometries, it is necessary to calculate the stress intensity factors for the geometries of interest, to obtain a relationship between the critical values of K_I, K_{II} and K_{III}, and to determine the direction of crack propagation. Such calculations may be carried out by finite element methods as shown in the paper, use being made of virtual crack extension methods. The relationship and direction of propagation has to be determined experimentally for each material of interest at each relevant temperature. However, a number of such relationships have been proposed on the basis of simplified assumptions, and in particular the virtual crack extension method described determines the change in energy for small tip displacements by a fixed amount in varied directions around the tip. A natural alternative to these previous simplified assumptions is the possibility that the crack begins to propagate at a critical value of this quantity and does so in that direction corresponding to the maximum energy change. However, even when this assumption is inappropriate for the material of interest, the results of the present investigations may be used to relate the stress intensity factors to the energy release rates when angles of propagation are known from experiments.

Stress intensity factors at the tips of two-dimensional cracks under asymmetric loading may be determined from the results of a finite element stress analysis either by a comparison

of the value of displacements near the crack tip with those of the known analytic solutions for a crack under uniform tension or by calculating the strain energy for a number of sizes of crack in order to determine its rate of increase as a function of crack size. Pian and Pin Tong [1] have recently proved that the rate of convergence as the element size decreases is greater for the strain energy release rate method. Rice [2] showed that the energy release rate for a two-dimensional crack extending in its plane in a homogeneous material was equal to a path independent integral J formulated by Eshelby [3] and applied to crack problems by Cherepanov [4]. Knowles and Sternberg [5] subsequently generalised J to be a vector J_k corresponding to the energy release rate for movement in any direction of the crack edge. In the two-dimensional case one component is zero and it is still a path independent integral for contours around the tip provided the contour begins and ends at the tip in directions tangential to the faces. Budiansky and Rice [6] have shown how the formula may be simplified for a homogeneous isotropic material by use of the theory of functions of a complex variable.

The aims of this paper are to relate J to the stress intensity factors K_{I} and K_{II} for a two-dimensional crack in such a material, and to consider its relevance to theories of the angle at which a crack begins to propagate. Also a finite element analysis using virtual crack extension techniques is discussed and compared with the theoretical developments.

2. Theory of J_1 and J_2 integrals

For a two-dimensional crack

$$J_k = \int \{W n_k - T_i \partial u_i / \partial x_k\} \, \mathrm{d}s \tag{1}$$

where W is the energy, u_i the displacement components and T_i the components of traction. The contour touches each surface of the crack at the tip and contains no other singularity. For in-plane loading $J = J_1 - iJ_2$ may be written as

$$J = \int \left\{ i W \, \mathrm{d}\bar{z} - \bar{T} \frac{\partial \bar{D}}{\partial z} \, \mathrm{d}s - \bar{T} \frac{\partial D}{\partial z} \, \mathrm{d}s \right\} \tag{2}$$

where $z = x + iy$, $D = u + iv$ and $T = T_x + iT_y$ and a bar denotes the complex conjugate.

It is well known (see e.g. Green and Zerna [7]) that the stress components may be written as the second derivatives of the Airy stress function ϕ which satisfies the biharmonic equation and hence may be written as

$$\phi = z\bar{\Omega}(\bar{z}) + \bar{z}\Omega(z) - \int z \, \mathrm{d}\Omega(z) - \int \bar{z} \, \mathrm{d}\bar{\Omega}(\bar{z}) + \int \chi(z) \mathrm{d}z + \int \chi(\bar{z}) \mathrm{d}z \tag{3}$$

where $\Omega(z)$ and $\chi(z)$ are functions of z and

$$\int T \, \mathrm{d}s = -2i(\partial \phi / \partial \bar{z}) \tag{4}$$

Thus J simplifies to

$$J = \int \left\{ i W \, \mathrm{d}\bar{z} - 2i \frac{\partial D}{\partial z} \, \mathrm{d} \frac{\partial \phi}{\partial z} + 2i \frac{\partial D}{\partial z} \, \mathrm{d} \frac{\partial \phi}{\partial \bar{z}} \right\}. \tag{5}$$

By differentiating Eqn. (3) twice it is found that

$$\begin{aligned} \sigma_{yy} + i\sigma_{xy} &= 2\bar{\Omega}'(\bar{z}) + 2\chi'(z) + 2(\bar{z} - z)\Omega''(z) \\ \sigma_{yy} + \sigma_{xx} &= 4\bar{\Omega}'(\bar{z}) + 4\Omega'(z) \end{aligned} \tag{6}$$

and then on use of the stress-strain relationship and integrating, the displacement D can be expressed as

$$ED/[2(1+\nu)] = \kappa\Omega(z) - \bar{\chi}(\bar{z}) - z\bar{\Omega}'(\bar{z}) + \bar{z}\bar{\Omega}'(\bar{z}) \tag{7}$$

where E is Young's modulus, ν Poisson's ratio and κ is $3-4\nu$ for plane strain and $(3-\nu)/(1+\nu)$ for plane stress. Also the strain energy density

$$W = [(1+\nu)/E]\{\sigma_{xy}^2 + \tfrac{1}{4}(\sigma_{xx}-\sigma_{yy})^2 + \tfrac{1}{8}(\kappa-1)(\sigma_{xx}+\sigma_{yy})^2\}$$

becomes on use of Eqn. (6)

$$W = [[4(1+\nu)]/E]\{[\bar{\Omega}'(\bar{z}) + (\bar{z}-z)\bar{\Omega}''(\bar{z}) - \bar{\chi}'(\bar{z})][\Omega'(z) + (z-\bar{z})\Omega''(z) - \chi'(z)] + \tfrac{1}{2}(\kappa-1)[\Omega'(z) + \bar{\Omega}'(\bar{z})]^2\}. \tag{8}$$

On substitution from Eqns. (3), (7) and (8) in Eqn. (5) it becomes when written fully

$$\begin{aligned} J = {} & [[4i(1+\nu)]/E] \oint \{[\chi'(z) + (\bar{z}-z)\Omega''(z) - \Omega'(z)][\chi'(z) + (z-\bar{z})\bar{\Omega}''(z) - \bar{\Omega}'(\bar{z})]\,\mathrm{d}\bar{z} + \\ & + \tfrac{1}{2}(\kappa-1)[\Omega'(z) + \bar{\Omega}'(\bar{z})]^2\,\mathrm{d}\bar{z} - [\chi'(z) + (\bar{z}-z)\Omega''(z) - \Omega'(z)][\chi'(\bar{z}) + (z-\bar{z})\bar{\Omega}''(\bar{z}) - \bar{\Omega}'(\bar{z})]\,\mathrm{d}\bar{z} - \\ & - [\kappa\Omega'(z) - \bar{\Omega}'(\bar{z})][\Omega'(z) + \bar{\Omega}'(\bar{z})]\,\mathrm{d}\bar{z} - [\chi'(z) + (\bar{z}-z)\Omega''(z) - \Omega'(z)][\Omega'(z) + \bar{\Omega}'(\bar{z})]\,\mathrm{d}z - \\ & - [\kappa\Omega'(z) - \bar{\Omega}'(\bar{z})][\chi'(z) + (\bar{z}-z)\Omega''(z) - \Omega'(z)]\,\mathrm{d}z\} \end{aligned}$$

which reduces to

$$\begin{aligned} J &= [[2i(1+\nu)(1+\kappa)]/E] \oint \{[\Omega'^2(\bar{z}) - \Omega'(z)]\,\mathrm{d}\bar{z} - 2\Omega'^2(z)[\chi'(z) + (\bar{z}-z)\Omega''(z) - \Omega'(z)]\,\mathrm{d}z\} \\ &= [[2i(1+\nu)(1+\kappa)]/E] \oint \{\Omega'^2(z)\mathrm{d}z + \Omega'^2(\bar{z})\mathrm{d}\bar{z} - 2\Omega'(z)\chi'(z)\mathrm{d}z + \mathrm{d}[\Omega'^2(z)(z-\bar{z})]\} \end{aligned} \tag{9}$$

In most cases of interest (for example when the x axis is taken along the line of the crack) the final term is zero for a complete contour so that

$$J = [[4i(1+\nu)(1+\kappa)]/E]\{\mathrm{Re}\oint \Omega'(z)\mathrm{d}z - \int \Omega'(z)\chi'(z)\mathrm{d}z\}\,. \tag{10}$$

If the crack tip is chosen as origin (with the crack along part of the negative x axis) this may be evaluated by the residue theorem for integrals around the origin since the singular parts of $\Omega'(z)$ and $\chi'(z)$ at the origin are known to be

$$(K_{\mathrm{I}} + iK_{\mathrm{II}})/4(2\pi z)^{\frac{1}{2}} \text{ and } (K_{\mathrm{I}} - iK_{\mathrm{II}})/4(2\pi z)^{\frac{1}{2}} \text{ respectively} \tag{11}$$

where K_{I} and K_{II} are the stress intensity factors. Hence J may be determined on substitution from Eqn. (11) in Eqn. (10) as

$$J = \frac{(1+\nu)(1+\kappa)}{4E}(K_{\mathrm{I}}^2 + K_{\mathrm{II}}^2 + 2iK_{\mathrm{I}}K_{\mathrm{II}})\,. \tag{12}$$

Thus the values of energy release rate for crack extensions parallel and perpendicular to the crack are

$$J_1 = \frac{(1+\nu)(1+\kappa)}{4E}(K_{\mathrm{I}}^2 + K_{\mathrm{II}}^2) \text{ and } J_2 = -\frac{(1+\nu)(1+\kappa)}{2E}K_{\mathrm{I}}K_{\mathrm{II}} \tag{13}$$

while the maximum energy release rate is for a crack extending at an angle

$$\tan^{-1}[2K_{\mathrm{I}}K_{\mathrm{II}}/(K_{\mathrm{I}}^2 + K_{\mathrm{II}}^2)] \tag{14}$$

to the plane of the crack and has magnitude

$$\frac{(1+\nu)(1+\kappa)}{4E}\{K_I^4+6K_I^2K_{II}^2+K_{II}^4\}^{\frac{1}{4}}. \tag{15}$$

Of course in a real material the angle at which a crack begins to propagate is something which must be determined experimentally even in the homogeneous isotropic case. Nevertheless it is of interest to compare Eqns. (14) and (15) with the other criteria that have been derived for a linear elastic material. Griffith [8] considered a criterion based on the limit, as the minimum radius tends to zero, of the maximum surface stress for an elliptical hole. For a slit crack with cohesive stresses acting over the tip, this is equivalent to a limit on the magnitude of the traction at the tip. The maximum traction is acting normal to a direction making an angle with the plane of the crack of

$$\tfrac{1}{2}\tan^{-1}K_{II}/K_I \tag{16}$$

and thus a limit on its magnitude implies a limit to

$$\tfrac{1}{2}K_I+\tfrac{1}{2}(K_I^2+K_{II}^2)^{\frac{1}{2}}. \tag{17}$$

An alternative maximum stress criterion (Erdogan and Sih [9]) imposes a restriction on the magnitude of the coefficient of the singular part of the stress near the tip of the slit in the absence of cohesive stress. They show that this occurs at an angle θ with the plane of the crack such that

$$K_I\sin\theta+K_{II}(3\cos\theta-1)=0 \tag{18}$$

and a limit on the magnitude is a limit on

$$\frac{\{2K_I+6\sqrt{(K_I^2+8K_{II}^2)}\}K_{II}^3}{\{\frac{1}{4}K_I^2+3K_{II}^2-\frac{1}{4}K_I\sqrt{(K_I^2+8K_{II}^2)}\}^{\frac{3}{2}}}. \tag{19}$$

3. Virtual crack extensions using finite elements

The calculation of stress intensity factor using finite element techniques has been studied widely. Several methods are now known for deriving K from the results, using either the local crack tip equations or energy methods as investigated by Iida *et al.* [10] and Watwood [11] respectively. Recent review papers include Rice and Tracey [12] and Jerram and Hellen [13]. The substitution methods generally give K_I and K_{II} separately but are not particularly accurate or easy to use, whereas the energy methods require extra assumptions to segregate K_I and K_{II}. Direction finding is tedious, requiring either many computer resubmissions or investigation of the local tensile stresses, which are not accurately computed.

The use of virtual crack extensions for calculating energy release rates avoids these problems. By considering the derivative of potential energy in only the elements containing the crack tip, as suggested by Rice (private communication), and using an efficient procedure for compiling the strain energy difference in these elements with the tip in the original position and a slightly different position (a virtual extension), a number of energy release rates can be determined in one computer submission (Hellen [14]). The computation is efficient in that each new extension considered enables an immediate calculation of energy release rate, and adds only a few percent onto the running time. Any direction or length of virtual extension can be considered and the results are known before the stage when the overall displacements and stresses are calculated. The technique has been inserted in the BERSAFE stress analysis (Hellen [15]) and is applicable to all two- or three-dimensional

structures with mechanical and thermal loads outside the crack tip elements. Consistent results arise from virtual extensions of different magnitudes in the same direction, although for extremely small or large extensions compared with the crack tip element size errors due to round off and mesh distortion respectively appear.

By considering a circle of virtual extensions around the tip in mixed mode cases, the maximum energy release rate resulting, corresponding to J in the previous section, can be determined together with the associated angle. A further computer submission may be required to find the angle and J value more accurately. The values of J_1 and J_2 can be calculated by using virtual crack extensions ahead of and perpendicular to the crack direction.

A further gain in accuracy for a given finite element mesh is the use of special shape functions in the elements containing the crack tip. Shape functions which give displacement varying s $r^{\frac{1}{2}}$ and as r radially away from the tip are used, with linear and quadratic variations in other directions [16]. In two-dimensions (plane or axisymmetric) such elements exist in BERSAFE for compatability with linear or quadratic isoparametric elements, and in three-dimensions for quadratic isoparametric elements. These elements, when used with virtual crack extension techniques, give particularly accurate results, and this combination (with quadratic elements) has been used for the following examples.

4. Slanting crack under uniaxial tension

The effect of crack angle on direction of maximum energy release rate was investigated using an oblique crack in a plate subjected to tensile loading (Fig. 1). Erdogan and Sih [9] have investigated the problem theoretically and experimentally, using plexiglass, for a range of angles. Their theory was based on the assumption that the direction of propagation was normal to the maximum tensile stress, which resulted in a relationship between θ and β (Fig. 1) of the form

$$\sin\theta + (3\cos\theta - 1)\cot\beta = 0\,. \tag{20}$$

The current theory developed in Section 2 gives a value for θ as based on the maximum energy release rate criterion. This is close to Eqn. (20) for values of $\beta \geqq 60°$, but as β approaches zero, the two forms diverge.

In order to enable a range of angles to be analysed with minimal effort, a mesh based on

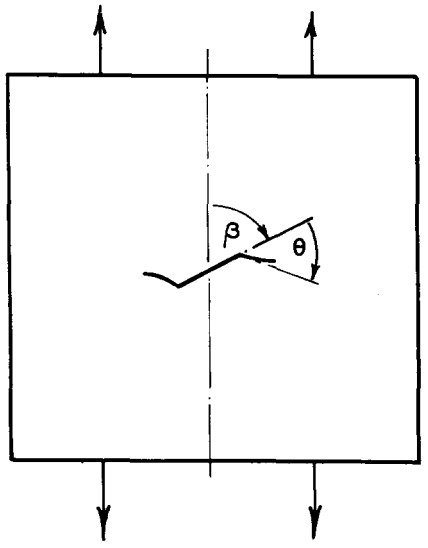

Figure 1. Slanting crack in tensile strip.

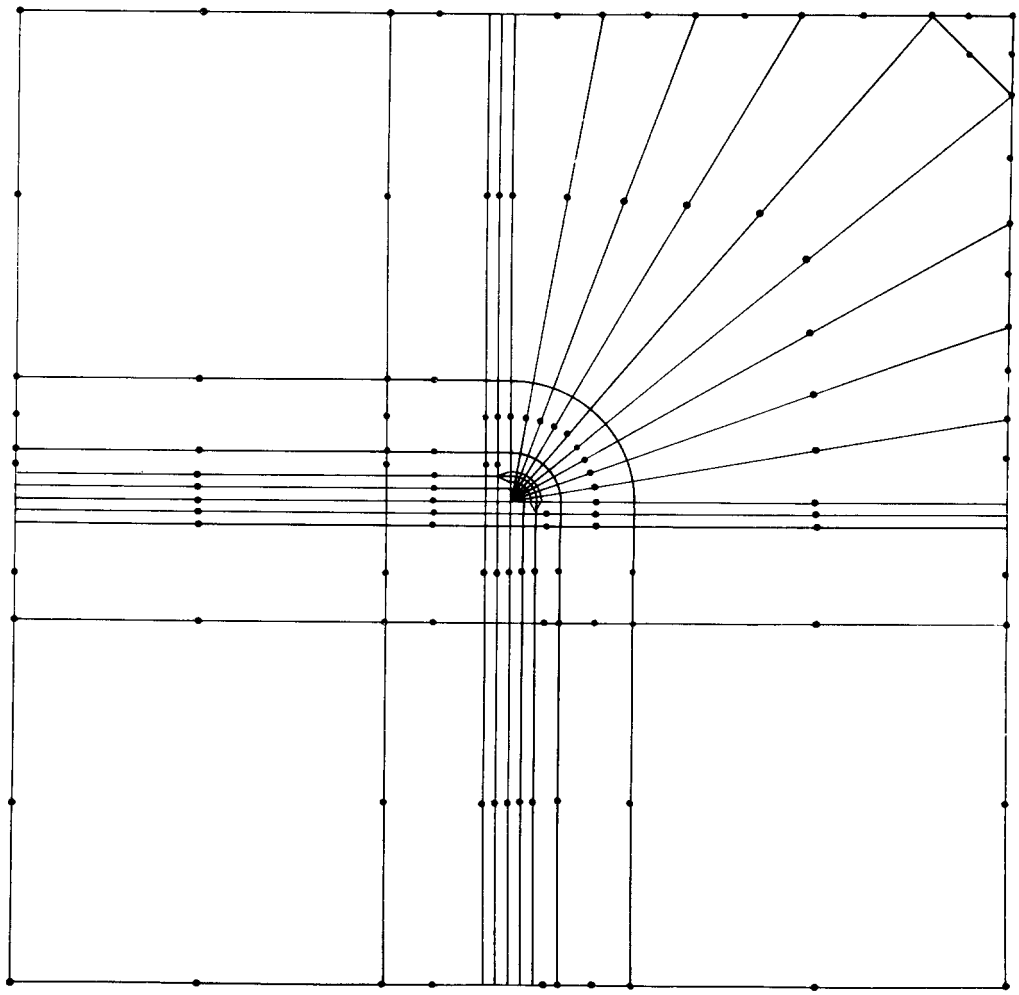

Figure 2. General mesh for slanting crack problem.

rays of lines from the centre of the square plate was designed. The crack was assumed to start at the centre and, at its other end, a local refinement was made for each angle investigated. The crack itself was effected by using the BERSAFE decoupling facility making nodes along the crack take double values for each side. Although the centre of the crack was slightly offset from the centre of the plate, the plate size was 20 times the crack length and so no inaccuracies were envisaged. Also, the end of the crack at the centre of the plate had no refinement there, but again this was not expected to affect the results at the refined end of the crack. The overall mesh is shown in Fig. 2, with a refinement around the crack tip for $\beta = 60°$ shown in Fig. 3. The crack extends from nodes A to B.

For $\beta = 60°$, several variations were attempted to investigate the quality of the results. Firstly, the direction of propagation was varied around 360° (Fig. 4) and a sinusoidal variation of G resulted. The maximum value of G corresponded to 99°, measured round from the direction of loading, a result which agrees closely with alternative results (see below). The minimum value of G is 180° out of phase and is the negative of the maximum value, showing an energy gain rate. The crack cannot, from energy considerations, go in this direction. G is zero at the two points in between these two angles, at 8° and 188°, showing that propagation in that direction would yield no energy release rate, an impossible situation. Corresponding to the maximum value of 99°, where the crack was assumed to propagate,

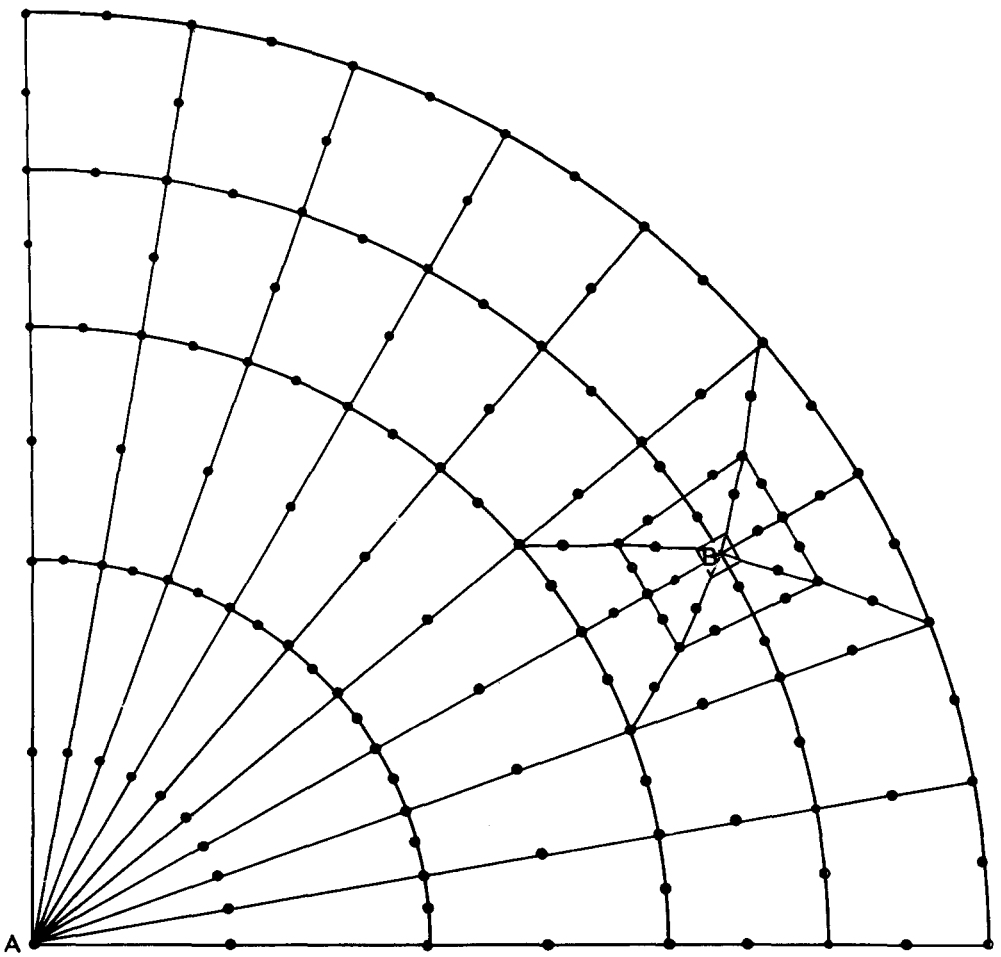

Figure 3. Detail of crack refinement when $\beta = 60$.

several different lengths of virtual crack extension δa were tried in evaluating G. δa values of 0.5, 0.05, 0.005 and 0.00005 of the tip element size produced very consistent values of G, the total variation being only 4%.

Values of Poisson's ratio equal to 0, 0.3 and 0.45 were tried to test the predicted effects on various materials, but negligible differences occurred in all results. Hence the computed results can be assumed to hold for plexiglass type material, where $\nu = 0.38$.

In order to investigate the accuracy of the finite element mesh and its local tip refinement adopted in Figs. 2 and 3, a more refined local region was designed with twice as many elements circumferentially and an extra layer radially about the tip. This extra refinement was made on two of the angles for which the results were likely to be the least accurate, $\beta = 20°$ and the shear case. Nevertheless, results obtained were within 1 or 2% of those from the standard mesh, so it was concluded that the standard mesh was adequate for this problem.

Figure 5 shows a graph of θ plotted against β, θ being the angle of propagation measured from the direction of the crack. Comparisons with Erdogan and Sih's theoretical and experimental results are shown, together with Eqn. (2) herein. Experimental results for the same material have been obtained by Williams and Ewing [17] and show little variation from Ref. 9. Pook [18] has given results for an aluminium alloy and these are also included. Iida and Kobayashi [10] noted that slanted cracks at angles of 30° and 45° in an aluminium alloy began to propagate under cyclic loading in directions almost normal to that of the

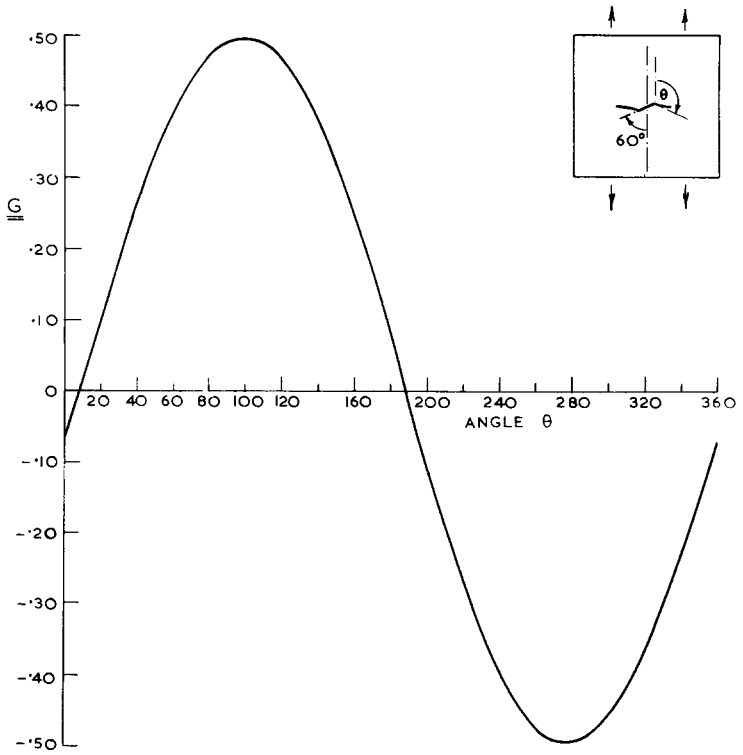

Figure 4. Crack slanting at 60° to uniaxial tensile field: Plot of G against angle with constant extension length of 0.05 of tip element size.

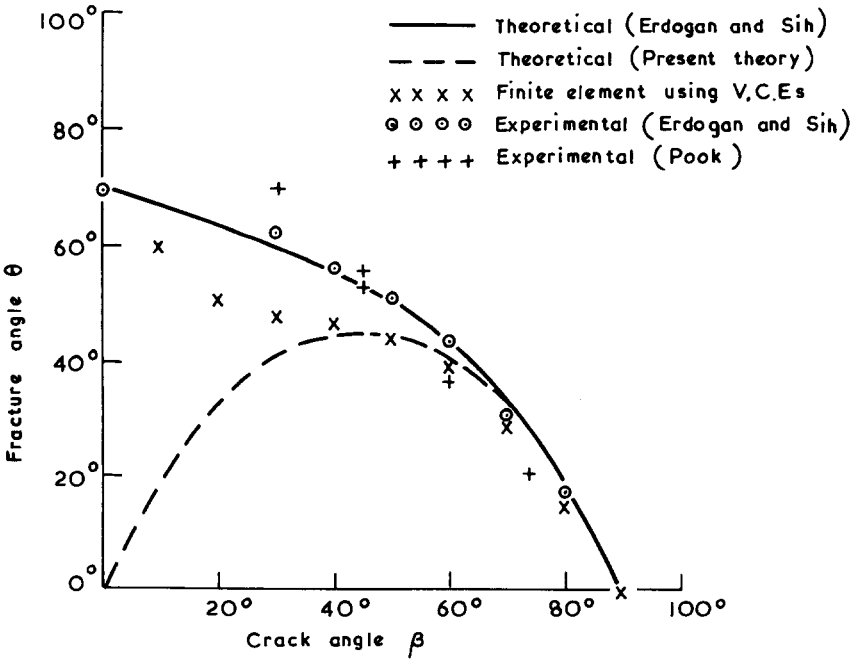

Figure 5. Fracture angle against crack angle in a cracked plate in tension.

applied load and subsequently propagated in directions such that K_{II}/K_I was small.

Figure 6 shows the values of the maximum energy release rate for the different crack slopes, and shows a rapid decrease as the crack becomes parallel to the direction of loading. Thus, in order to initiate propagation, more load is required as β decreases and so for the experimental cases, plasticity effects start to appear. It is likely that for low angles of β, considerably plasticity is present, invalidating the linear theories. Hence, comparisons with low values of β should be treated with caution. All results agree well for angles of 60° and above, the some divergence occurs, of limited amount, down to $\beta = 40°$. After that, considerable divergence occurs but the plastic effects render experimental evidence somewhat doubtful.

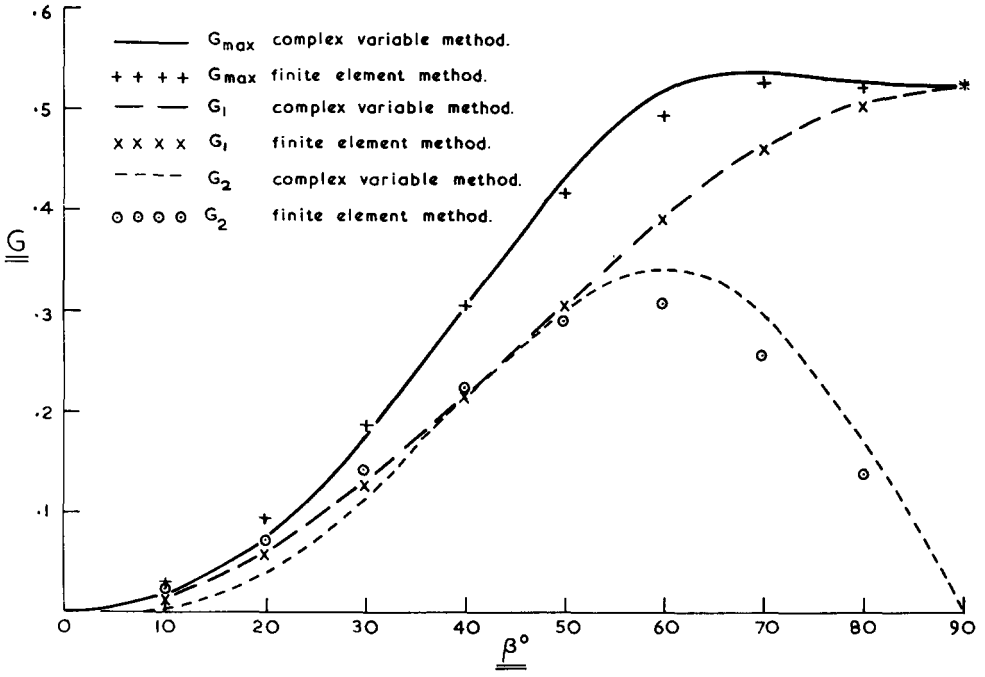

Figure 6. Values of energy release rates for various angles of slanting crack.

Where experimental results have been obtained [9, 17, 18], if the measured critical values of $\{1+6K_{II}^2/K_I^2+K_{II}^4/K_I^4)^{\frac{1}{2}}$ were to be scaled by the value of G for $\beta = 90°$ and superimposed on Fig. 6, they would lie above the curve for G, thus suggesting that the maximum energy release rate criterion is inappropriate for these materials. Figure 6 also shows the energy release rates for crack extension in the plane of (G_1), and perpendicular to (G_2), the plane of the crack, compared with $\pi a\sigma^2 \sin^2 \beta/E$ and $2\pi a\sigma^2 \sin^3 \beta \cos \beta/E$ as predicted from Eqn. (13).

A noteworthy result illustrated in Fig. 6 is that the maximum energy release rate occurs when β is approximately 70°. This may be predicted from Eqn. (15) with $K_I = \sigma(\pi a)^{\frac{1}{2}} \sin^2 \beta$ and $K_{II} = \sigma(\pi a)^{\frac{1}{2}} \cos \beta \sin \beta$ where σ is the stress and a the half length of the crack. Then the maximum energy release rate is $(\pi a\sigma^2)/E \sin \beta[(1+\sin^2 2\beta)^{\frac{1}{2}}]$ which has its maximum when $\sin^4 \beta + 4 \sin^6 \beta - 4 \sin^8 \beta$ does. By differentiating this with respect to $\sin^2 \beta$ this is found to occur when $\sin^2 \beta = [3+\sqrt{17}]/8$, or $\beta = 70.6°$.

As β tends to zero, K_I/K_{II} tends to zero. Therefore to avoid errors due to the differences in refinement at the ends when all the stresses are small, a run was carried out with the same mesh as for β equal to 90° but with equal and opposite point loads applied tangentially at the centre of the crack, in order to obtain a case where K_I/K_{II} is zero. The angle for maximum energy release was found to be 1° (as compared with 0° predicted from Eqn. (14)).

5. Propagating crack in an arbitrary structure

A further example is given of a fatigue crack propagating in a channelled specimen from a small spark-machined notch. Experimental results due to Jerram [19] give a curving crack profile extending approximately half-way through the specimen after a large number of cycles. Since the angle of propagation is not large, the K_I mode dominates, and it is shown that the maximum energy release rate criterion using virtual crack extensions gives almost identical results to the maximum tensile stress criterion of Erdogan and Sih [9] and the observed experimental results.

The range of stress intensity factor, ΔK, is the primary parameter governing crack propagation. Formulae of the form

$$da/dN = C(\Delta K)^4$$

were suggested by Paris and Erdogan [20] from observations on published data, a being the crack length and N the number of cycles.

Theoretical approaches therefore require computation of the stress intensity factor as a function of crack length.

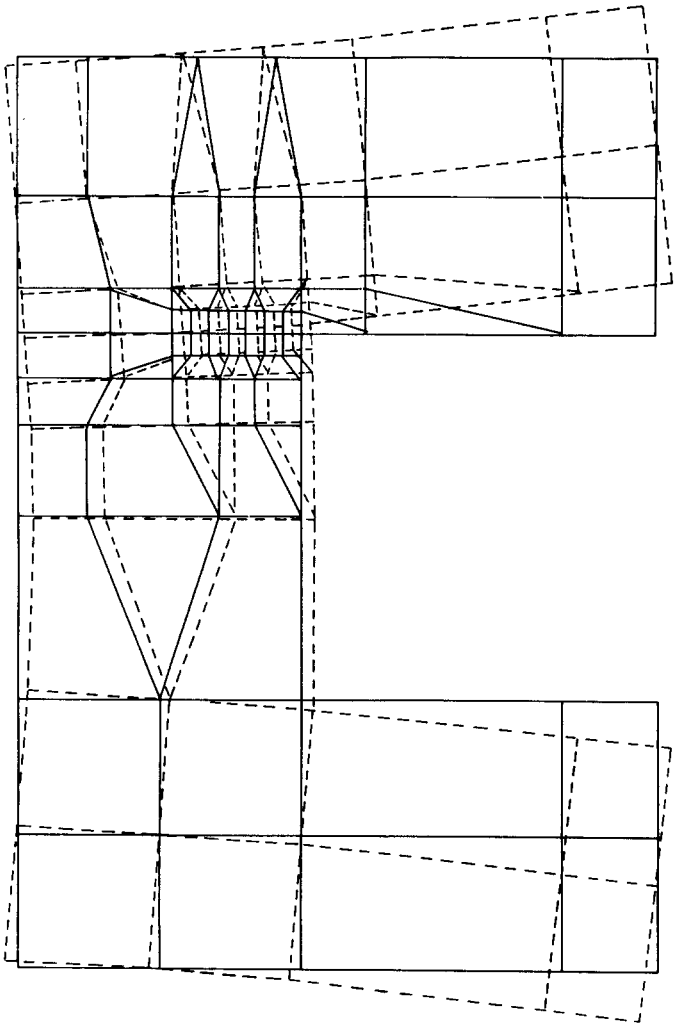

Figure 7. Finite element mesh and deformation plot with no crack in specimen.

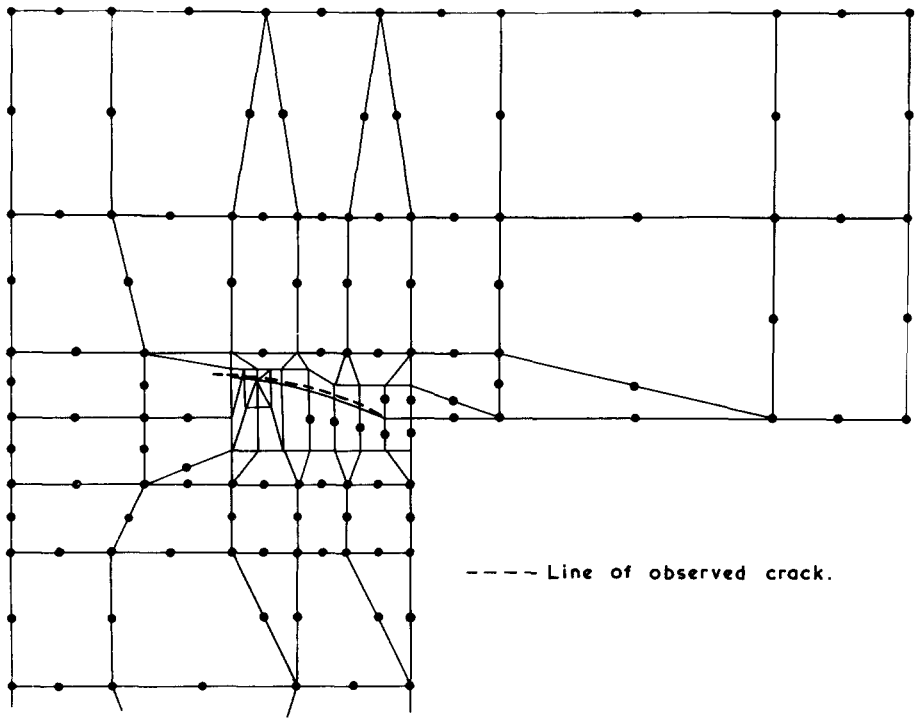

Figure 8. Mesh at longest crack position analysed.

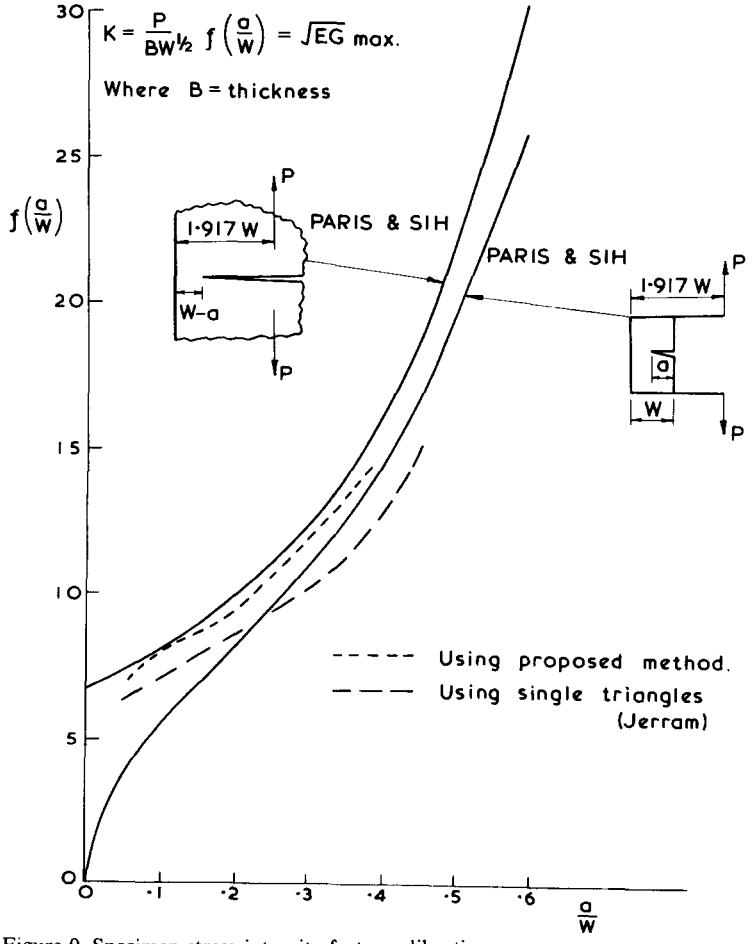

Figure 9. Specimen stress intensity factor calibrations.

A mesh of quadratic isoparametric elements was designed, initially with no crack, and is shown in Fig. 7 together with a deformation plot when loaded at the centre of the holes used in the experiments. The mesh was designed with fairly small elements in the crack region such that the crack growth could be followed in increments equal to the width of these local elements. Around each successive tip, a local refinement was made with the innermost elements having special singularity shape functions.

The crack was allowed to grow by using the decoupling facility available in BERSAFE.

Six tip positions were used altogether. The $a:w$ ratio was calculated using the horizontal component of crack length to be consistent with Jerram [19]. Each successive tip had a local refinement as at the first tip, the sixth being shown in Fig. 8. The superimposed dotted line shows the crack path observed on the specimen. Jerram [19] assumed the crack path from the specimen and observed that the direction of maximum principal stress at each successive tip was always perpendicular to the path there.

The value of $K=(EG)^{\frac{1}{2}}$ is shown in Fig. 9. Since K_{II} is present, K represents $(K_I^4+6K_I^2K_{II}^2+K_{II}^4)^{\frac{1}{4}}$. Results computed by Jerram [19] using simple triangles are included and are lower since they are less accurate than the present technique. Two models from Paris and Sih [21] are included which are expected to bound the actual specimen results. One model is a semi-infinite notch at the free edge of a half-plane, resembling the upper side of the specimen crack, and the other is an edge-notched strip resembling the lower side of the specimen crack. Both models have horizontal cracks but are seen to bound the new results in the entire range. As the crack grows, the edge strip model is approached as would be expected. The simple triangle results are not entirely bounded due probably to inaccuracies in using these elements.

6. Discussion and conclusions

It is concluded that the method of virtual crack extension is an appropriate way for calculating the energy release rate for combined tensile and shear loading in two dimensions. Also, its magnitude for crack extension at an arbitrary angle can be calculated accurately from its values for crack extension in and perpendicular to the crack plane. From the former of these may be determined $K_I^4+6K_I^2K_{II}^2+K_{II}^4$ and from the ratio of the latter to the former (which is tan θ where θ is the angle at which the crack propagates) the ratio of K_{II} to K_I may be determined by use of Fig. 5.

Calculations of the path independent integrals J_1 and J_2 by use of functions of a complex variable agree well with the numerical calculations of energy release rate by a virtual crack extension method except for J_2 when K_{II} is greater than K_I.

For a brittle material in which plasticity effects are negligible, the foregoing work may be construed as a theory for predicting the angle at which a crack would propagate under combined tensile and shear loading on the assumption that there is a critical value for the change in energy when the position of the end of the crack changes by a fixed amount and that the crack propagates in that direction for which this change is a maximum. Thus it forms an alternative to the theories of Griffith and of Erdogan and Sih. The experimental evidence available does not confirm such a theory where signifigant differences between the various theories exist, i.e. when shear is more significant than tension. However for these cases the effects of plasticity would be more significant. According to this theory a crack in shear extends in its plane. Also a crack of given length under a uniaxial applied stress at infinity begins to extend most readily when the direction of the stress is at about 20° to the normal to its plane (β approximately 70°).

Whether or not one accepts such a theory however, the results of Figs. 5 and 6 may be used to determine K_I and K_{II} from calculations of virtual crack extension in two orthogonal directions (preferably parallel and perpendicular to the crack).

Acknowledgement

The authors are grateful to the Central Electricity Generating Board and the Directors of C.A. Parsons and Co. Ltd. for permission to publish this paper. Part of the work was sponsored by a Power Engineering Research Steering Committee Contract.

REFERENCES

[1] Pin Tong and T. H. H. Pian, On the convergence of the finite element method for problems with singularities, *Int. Jnl. Solids and Struct.*, 9 (1973) 313–321.
[2] J. R. Rice, A path independent integral and the approximate analysis of strain concentration by notches and cracks, *Jnl. Appl. Mech.*, 34 (1968) 379–386.
[3] J. R. Eshelby, The continuum theory of lattice defects, *Solid State Physics*, 3 (1956).
[4] G. L. Cherepanov, Cracks in Solids, *Prikl. Math. Mekh.*, 25 (1967) 476–488.
[5] J. K. Knowles and E. Sternberg, On a class of conservation laws in linearised and finite elastostatics, *Arch. Rat. Mech. Anal.*, 44 (1972) 187–211.
[6] B. Budiansky and J. R. Rice, Conservation Laws and Energy Release Rates, *Jnl. Appl. Mech.*, 40 (1973) 201–205.
[7] A. E. Green and W. Zerna, *Theoretical elasticity*. Oxford Univ. Press. 1954.
[8] A. A. Griffith, The phenomenon of rupture and flow in solids, *Proc. 1st. Int. Congr. Appl. Mech.*, 1924.
[9] F. Erdogan and G. C. Sih, On the crack extension in plates under plane loading and transverse shear, *Jnl. Basic Eng.*, 85 (1963) 519–527.
[10] S. Iida and A. S. Koboyashi, Crack propagation rate in 7075-T6 plates under cyclic tensile and transverse shear loadings, *Jnl. Basic Eng.*, 91 (1969) 764–769.
[11] V. B. Watwood, *Nucl. Eng'g. Design*, 11 (1969) 323–332.
[12] J. R. Rice and D. M. Tracey, Computational Fracture Mechanics, in *Numerical and Computer Methods in Struct. Mechs.*, Academic Press, N.Y. (1973).
[13] K. Jerram and T. K. Hellen, *Finite Element Techniques in Fracture Mechanics*, Int. Conf. on Welding Research related to Power Plant, Southampton (1972).
[14] T. K. Hellen, *The Finite Element Calculation of Stress Intensity Factors using Energy Techniques*, Conf. Struct. Mechs. in Reactor Tech., Berlin (1973).
[15] T. K. Hellen, *The Application of the BERSAFE Finite Element System to Nuclear Design Problems*, Conf. Struct. Mechs. in Reactor Tech., Berlin (1971).
[16] W. S. Blackburn, *Calculation of Stress Intensity Factors at Crack Tips using Special Finite Elements*, Conf. Mathematics of Finite Elements and Applications, Brunel University (1972).
[17] J. G. Williams and P. D. Ewing, Fracture under complex stress the angled crack problem, *Int. J. Fract. Mech.*, 8 (1972) 441–446.
[18] L. P. Pook, The effect of crack angle on fracture toughness, *Eng. Fract. Mechs.* 3 (1971) 205–218.
[19] K. Jerram, C.E.G.B. Report RD/B/N 1777 (1970).
[20] P. C. Paris and F. Erdogan, *Jnl. Basic Eng.*, 85 (1963) 528–534.
[21] P. C. Paris and G. Sih, *Fracture Toughness Testing and Its Applications*, ASTM Special Technical Publication No. 381, Philadelphia (1965) 30–81.

RÉSUMÉ

On présente des calculs de l'intensité des contraintes dans les cas de mises en charge combinée par traction et cisaillement d'un matériau redevable de la mécanique linéaire et élastique. En utilisant des fonctions d'une variable complexe, on développe une théorie pour la détermination de la direction du taux maximum de relaxation de l'énergie. Une méthode par éléments finis utilisant des extensions d'une fissure virtuelle est également employée pour déterminer le taux de relaxation de l'énergie correspondant à des extensions de la fissure dans des directions diverses et, en particulier, dans celle qui donne un taux de relaxation maximum de l'énergie.

A l'exception du cas où le cisaillement est significativement plus important que la traction, les résultats sont en bon accord avec les observations expérimentales. Lorsque le cisaillement est proportionnellement le plus significatif, les effets de la plasticité deviennent probablement importants, et rendent invalides les résultats de toute théorie élastique linéaire. Toutefois, la méthode peut être encore utilisée pour la détermination numérique de K_I et K_{II} au départ de calculs de J_1 et J_2 correspondant à une extension d'une fissure virtuelle dans des géométries bidimensionnelles.